GREEN SYNTHESIS AND CHARACTERIZATION OF MgO-MnO-BIOCHAR TERNARY NANOCOMPOSITE FOR POTENTIAL HEAVY METAL REMEDIATION

BY

COURAGE ENUESUEKE

PSC2007976

SUBMITTED TO THE DEPARTMENT OF CHEMISTRY

FACULTY OF PHYSICAL SCIENCE

UNIVERSITY OF BENIN

BENIN CITY

FEBRUARY, 2025

GREEN SYNTHESIS AND CHARACTERIZATION OF MgO-MnO-BIOCHAR TERNARY NANOCOMPOSITE FOR POTENTIAL HEAVY METAL REMEDIATION

BY

COURAGE ENUESUEKE

PSC2007976

A PROJECT REPORT SUBMITTED TO THE DEPARTMENT OF CHEMISTRY, FACULTY OF PHYSICAL SCIENCE IN PARTIAL FUFILMENT OF THE REQUIREMENT OF A BACHELOR'S DEGREE IN CHEMISTRY (PURE) IN THE UNIVERSITY OF BENIN, BENIN CITY

FEBRUARY, 2025

CERTIFICATION

This is to certify that the project work was carried out by COURAGE ENUESUEKE with the matriculation number PSC2007976 in partial fulfillment of the requirement of the award of B.Sc. (Hons) Degree of Pure Chemistry.

_____ _____

COURAGE ENUESUEKE DATE
(PROJECT STUDENT)

_____ _____

PROF. J. M. OKUO DATE
(PROJECT SUPERVISOR)

_____ _____

PROF. E.E. IRABOR DATE
(HEAD OF DEPARTMENT)

DEDICATION

I dedicate this project to the countless individuals whose support, guidance, and inspiration have been the driving force behind its completion. To my beloved family, whose unwavering love and encouragement have been my guiding light and greatest source of strength and motivation through every twist and turn of this journey, your sacrifices and belief in me have fueled my determination to excel. To my esteemed professors, doctors, and mentors, whose wisdom, invaluable guidance, and encouragement have shaped my academic growth and instilled in me the courage to pursue excellence. To my cherished friends, whose unwavering support, camaraderie, and laughter have brightened my darkest days and made this journey unforgettable. To all the participants and contributors of this research, whose invaluable insights, cooperation, and willingness to share their knowledge have enriched this project and contributed to its success. And finally, to myself, for the resilience, perseverance, and hard work that have propelled me forward, overcoming obstacles and reaching new heights. May this project serve as a testament to the collective effort, passion, and commitment of all who have played a part in its realization.

ACKNOWLEDGEMENT

I would like to express my deepest gratitude to Jehovah for seeing me through this tasking phase of my academics and to all who contributed to the completion of this undergraduate project.

First and foremost, I am immensely thankful to my supervisors, Prof. J.M. Okuo and Dr. (Mrs) Oluchi Emeribe, for their invaluable guidance, mentorship, and support throughout this project. Their expertise, encouragement, and constructive feedback have been instrumental in shaping the direction and outcome of this research.

I am also grateful to the members of the Department of Chemistry for their academic guidance, insightful discussions, and willingness to share their knowledge and expertise. Their dedication to teaching and research has been a constant source of inspiration.

I extend my heartfelt appreciation to the participants and contributors of this study, particularly to Marvellous Eyube for his invaluable contribution. Your cooperation, insights, and willingness to share your expertise have greatly enriched the quality and depth of this project.

I am indebted to my family for their unwavering love, encouragement, and understanding throughout my academic journey. Their support has been a pillar of strength, motivating me to overcome challenges and strive for excellence.

To all those mentioned above and to everyone else who has contributed in any way, I offer my sincere gratitude. Your support and encouragement have been invaluable, and I am truly thankful for the opportunity to undertake this project.

ABSTRACT

In today's world, the rise of modernization and industrialization has quietly reshaped ecosystems—the rapid expansion of industries and unchecked urbanization continue to disrupt fragile environments, leading to the persistent challenge of heavy metal contamination in soil. This study investigates the green synthesis and characterization of an MgO-MnO-biochar ternary nanocomposite as well as the MgO-MnO Nanopparticle using an eco-friendly co-precipitation method, and highlightening its potential heavy metal remediation applications. The synthesis involved the bottom-up fabrication of magnesium and manganese oxides in a green solvent system, followed by integration with biochar. The characterization of the MgO-MnO-biochar nanocomposite and MgO-MnO nanoparticle system revealed significant structural, compositional, and morphological differences. FTIR analysis showed the nanocomposite had prominent O–H stretching at 3951.1, 3641.1, and 3790.2 cm^{-1}, C–H stretching at 2907.3 cm^{-1}, CO_2 adsorption at 2110.3 cm^{-1}, C=C stretching at 1611.8 cm^{-1}, and Mg–O and Mn–O bonds at 946.3 and 864.7 cm^{-1}, while the nanoparticle system exhibited fewer functional groups, with CO_2 adsorption at 2102.2 cm^{-1} and C=C stretching at 1598.5 cm^{-1}. EDX analysis revealed high carbon content (48.72 wt%) in the nanocomposite, absent in the nanoparticle system, alongside higher Mn (61.62 wt%) and Mg (32.24 wt%) concentrations in the nanoparticle system compared to 24.47 wt% Mn and 11.34 wt% Mg in the composite. XRD analysis identified Lindergerbite (59.00%) and Periclase (13.00%) in the nanoparticle system, while the nanocomposite featured Flagstaffite (52.40%), Graphite (1.84%), and Cryoptohalite (7.96%). BET analysis showed the nanoparticle system had a higher surface area (282.000 m^2/g vs. 216.400 m^2/g), pore volume (0.173 cm^3/g vs. 0.128 cm^3/g), and BJH surface area (354.200 m^2/g vs. 265.400 m^2/g), though pore diameters were similar (2.132 nm vs. 2.129 nm). SEM analysis revealed the nanocomposite's porous, fibrous structure with well-dispersed nanoparticles, while the nanoparticle system exhibited a denser, more aggregated morphology with reduced porosity. The characterization results revealed that the MgO-MnO-biochar ternary nanocomposite possesses significant structural and compositional properties, suggesting its potential as a sustainable, cost-effective material for future heavy metal remediation applications.

Table of Contents

LIST OF TABLES

LIST OF FIGURES

CHAPTER ONE

INTRODUCTION AND LITERATURE REVIEW

1.1 Introduction

In the 21st century, the world is grappling with an unprecedented environmental crisis, where soil contamination with heavy metals has emerged as one of the most pressing concerns. As industries expand and urban sprawl intensifies, the delicate balance of our ecosystems is disrupted by the accumulation of toxic pollutants in the very ground that sustains life. These heavy metals, which include lead, cadmium, and arsenic, zinc, seep into the soil, entering food chains and posing significant risks to human health and biodiversity. As the scope of contamination grows, so does the urgency to find effective and sustainable solutions to remediate these pollutants.

Nanotechnology, with its ability to manipulate matter at the atomic and molecular levels, provides a powerful tool for soil decontamination. Research has demonstrated its potential to offer sustainable solutions for the remediation of heavy metals in soils, enhancing the efficiency of traditional techniques by improving the selectivity, reactivity, and mobility of treatment agents (Ekrami *et al.,* 2022). Among the most promising innovations is the development of nanocomposites that combine the strengths of various materials, such as magnesium oxide (MgO), manganese oxide (MnO), and biochar, to synergistically remove pollutants from contaminated environments. These advanced materials harness the unique properties of nanoparticles, which are significantly more reactive than bulk substances, thus increasing the efficiency of metal ion adsorption and reducing environmental impacts (HELAL *et al.,* 2016).

The application of nanotechnology in soil remediation has been a focal point of numerous studies, especially regarding the removal of heavy metals such as lead, cadmium, and arsenic, which are among the most hazardous and widespread contaminants. These metals, often resulting from agricultural runoff, industrial activities, and improper waste disposal, are not only toxic to plants and animals but also pose significant risks to human health, including kidney damage, carcinogenesis, and neurological disorders (Wuana and Okieimen, 2011). By employing nanocomposite materials, it becomes possible to target and extract these metals with high specificity, offering a much-needed solution to the contamination crisis.

As we move toward more sustainable practices, integrating MgO-MnO-biochar nanocomposites into soil remediation strategies holds immense promise. These materials not only contribute to the effective sequestration of toxic metals but also enhance the overall soil health, facilitating the restoration of ecosystems and the promotion of agricultural productivity. The combination of nanotechnology and biochar, for instance, has shown exceptional results in reducing the bioavailability of heavy metals, effectively neutralizing pollutants while simultaneously enriching the soil with carbon, which is vital for maintaining soil fertility and microbial activity (HELAL *et al.,* 2016). This innovative approach offers a holistic solution, capable of addressing the root causes of soil degradation while promoting ecological balance and sustainability as such, this study is aimed at investigating the effectiveness of MgO-MnO-Biochar ternary nanocomposite in the remediation of selected heavy metals from contaminated soil.

1.1.1 Background of Study

Soil contamination with heavy metals, such as lead (Pb), cadmium (Cd), chromium (Cr), and arsenic (As), has become a major environmental concern due to industrialization, agriculture, and urbanization, posing long-term ecological and health risks (Xiang et al., 2021; Bharti and Sharma, 2022). These metals disrupt soil microbial activity, reduce fertility, and threaten food safety, while exposure can cause neurological damage, organ dysfunction, and increased cancer risk (Zaynab et al., 2022).

Traditional remediation methods like soil washing, immobilization, and phytoremediation often fall short for highly mobile metals (Wang et al., 2022). Nanotechnology offers a promising alternative, with metal oxide nanoparticles such as magnesium oxide (MgO) and manganese oxide (MnO) showing high adsorption capacities (Qian et al., 2020). When combined with biochar, these nanoparticles form a ternary nanocomposite that enhances heavy metal removal by leveraging biochar's porosity and the chemical affinity of metal oxides (Ganie et al., 2021).

The MgO-MnO-Biochar system enhances remediation through synergistic interactions, where MgO and MnO provide active adsorption sites, while biochar boosts surface area and pollutant binding. Studies on similar systems highlight improved metal removal via physical adsorption and chemical interactions (Ji et al., 2022). However, further research is needed to clarify component interactions, optimize synthesis, and assess long-term environmental impacts.

1.1.2 Problem Statement

Soil contamination from heavy metals like lead (Pb), cadmium (Cd), and chromium (Cr) has intensified due to industrialization, agricultural runoff, and urbanization, posing significant environmental and health risks (Yuan et al., 2021). These metals persist in soil, impairing fertility, disrupting microbial activity, and entering the food chain, endangering both human and animal health (Long et al., 2021). Major contributors include mining, manufacturing, and wastewater discharge, which further threaten groundwater and ecosystem stability.

Conventional remediation methods, such as soil washing and chemical stabilization, often fall short in addressing contamination in deeper soil layers and can be environmentally invasive or costly (ur Rehman et al., 2023). Nanotechnology offers a promising alternative, with nanoparticle-based strategies demonstrating efficient heavy metal removal due to their high surface area and reactivity (Yadav et al., 2024; Susaimanickam et al., 2024).). The combination of biochar with MgO and MnO nanoparticles enhances metal adsorption and retention, forming a ternary nanocomposite that not only remediates contaminated soils but also promotes long-term soil health and sustainability.

1.1.3 Significance of the Study

This study holds significant potential in advancing sustainable nanomaterial synthesis and characterization, particularly in the development of eco-friendly strategies for environmental applications. The use of *Ficus exasperata* (sandpaper leaf) extract as a green solvent in the synthesis of MgO-MnO-Biochar ternary nanocomposites represents a novel and sustainable approach to nanotechnology. The bioactive compounds present in *Ficus exasperata* act as natural

reducing and stabilizing agents, reducing the need for toxic chemical reagents, thereby promoting greener synthesis routes (Yuan *et al.,* 2021).

By focusing on the synthesis and characterization of the nanoparticles and the ternary nanocomposite, the study will provide a deeper understanding of the structural and morphological, characteristics of the material, which are critical for its potential applications in heavy metal remediation. The comprehensive characterization—using X-ray Diffraction (XRD), Scanning Electron Microscopy (SEM), Fourier Transform Infrared Spectroscopy (FT-IR), and Brunauer-Emmett-Teller (BET) surface area analysis—will offer valuable insights into the material's crystallinity, surface morphology, functional groups, and textural properties. These findings will be instrumental in optimizing the nanocomposite for future environmental remediation applications, ensuring its efficiency in adsorbing and immobilizing toxic metals like lead, cadmium, and mercury (Long et al., 2021).

Furthermore, the study contributes to the growing field of biochar-based nanocomposites by investigating the synergistic role of metal oxides and biochar in material design. Metal oxides such as magnesium oxide (MgO) and manganese oxide (MnO) are well-known for their adsorption and catalytic properties, while biochar enhances stability, surface area, and reactivity. Understanding how these components interact in a ternary system will provide a foundation for future research into multifunctional nanomaterials, potentially improving the effectiveness of heavy metal remediation technologies (Qian *et al.,* 2020).

Finally, this research supports the global push toward sustainable nanotechnology by integrating green chemistry principles into nanoparticle synthesis. The use of plant-based extracts aligns with eco-friendly practices, reducing environmental and health risks associated with

conventional synthesis methods. By demonstrating the feasibility of green synthesis for metal oxide-biochar nanocomposites, this study paves the way for future research in scalable, sustainable, and high-performance materials for environmental and industrial applications (Ganie *et al.,* 2021).

1.1.4 Scope of the Study

This study focuses on the green synthesis and characterization of a MgO-MnO-Biochar ternary nanocomposite using an eco-friendly co-precipitation method. The scope encompasses the entire process, starting from the collection, identification, and extraction of *Ficus exasperata* (sandpaper leaf) as a green solvent for nanoparticle synthesis. The synthesis includes two key stages: the formation of the MgO-MnO binary nanoparticle using the eco-friendly extract and the subsequent synthesis of the ternary nanocomposite by incorporating biochar through the co-precipitation technique.

The characterization phase involves advanced analytical techniques to determine the structural, morphological, and physicochemical properties of the synthesized materials. Functional group analysis will be conducted using Fourier Transform Infrared Spectroscopy (FT-IR), while the crystalline structure and surface morphology will be evaluated using X-ray Diffraction (XRD) and Scanning Electron Microscopy (SEM), respectively. Additionally, Brunauer-Emmett-Teller (BET) surface area analysis will be employed to assess the textural properties, including surface area, pore size, and volume. Finally, the study will culminate in the evaluation of the synthesized nanocomposite's potential for heavy metal remediation, providing insights into its environmental and industrial applications. This study will not include batch adsorption experiments, heavy

metal removal efficiency testing, or environmental applications, as the primary focus remains on synthesis and characterization.

1.1.5 Aim and Objectives of the Study

Aim: The aim of the study is to synthesize and characterize a green-synthesized MgO-MnO-Biochar ternary nanocomposite as well as MgO-MnO binary system using an eco-friendly co-precipitation method, with detailed structural, morphological and physicochemical analysis for potential heavy metal remediation applications. To achieve the aim above, the following objectives are put forward. To:

- collection, identification and extraction of the *Ficus exasperata* (sandpaper leaf).
- synthesis of the MgO-MnO Nanoparticle and MgO-MnO-Biochar ternary nanocomposite
- synthesize the binary nanoparticle MgO-MnO nanoparticle using eco-friendly green solvent.
- synthesize the ternary nanocomposite via co-precipitation.
- analyze the functional groups of the ternary and binary system through an advanced spectroscopy technique, Fourier Transform Infrared Spectroscopy (FT-IR).
- characterize the ternary nanocomposite as well as the binary nanoparticle through advanced analytical techniques, such as X-ray Diffraction (XRD) and Scanning Electron Microscopy (SEM).
- evaluate the textural properties of the ternary nanocomposite including surface area, pore size and volume using Brunauer-Emmett-Teller (BET) surface area analysis.
- analysis of results for potential heavy metal remediation.

1.2 Literature Review

1.2.1 Nanotechnology in Soil Remediation

Nanotechnology has emerged as a promising tool for soil remediation due to its unique properties, which allow nanoparticles to interact with contaminants at the molecular level. The small size, high surface area, and reactive nature of nanoparticles enable them to effectively target and neutralize harmful substances in the soil. As contaminants such as heavy metals, pesticides, and organic pollutants continue to threaten soil quality, the application of nanotechnology presents a highly efficient and eco-friendly alternative to traditional remediation methods (Qian *et al.,* 2020). Nanoparticle-mediated remediation can address a wide range of environmental challenges by enhancing the mobility and reactivity of remediation agents, which improves their ability to detoxify and restore contaminated soil.

The mechanisms through which nanoparticles remediate soil are diverse, with adsorption, precipitation, and ion exchange being the most prominent processes. Adsorption is the process by which nanoparticles bind to heavy metals and organic pollutants, thereby reducing their bioavailability and preventing further environmental harm. This mechanism relies on the high surface area and functional groups on the nanoparticle surface, which can effectively attract and hold contaminants. Precipitation, on the other hand, occurs when nanoparticles interact with pollutants to form insoluble compounds, which then settle in the soil, thus immobilizing the contaminants. This method reduces the risk of pollutants leaching into groundwater. Ion exchange, a process where nanoparticles swap their ions with those of the contaminants, helps in reducing the toxicity and mobility of harmful substances in the soil (Kristanti *et al.,* 2021).

Nanoparticles, particularly metal oxides such as magnesium oxide (MgO) and manganese oxide (MnO), have been shown to effectively adsorb heavy metals from contaminated soil. These metal oxide nanoparticles can form stable complexes with toxic ions, thus immobilizing them and preventing their spread into the environment. Their high surface reactivity and electrostatic interactions with pollutants make them ideal candidates for soil remediation (Rajput *et al.,* 2022). Additionally, the incorporation of biochar into nanoparticle-based remediation systems can enhance the stability and performance of these materials by providing a porous structure that adsorbs and holds contaminants, improving their retention in the soil (Bakshi and Abhilash, 2020).

The application of nanotechnology in soil remediation is not without its challenges and implications. While the potential benefits are clear, the long-term effects of nanoparticles on soil health, ecosystems, and human health remain a concern. The movement of nanoparticles in the soil, their interactions with soil microorganisms, and the possibility of bioaccumulation in the food chain are all factors that need to be carefully considered. Furthermore, the cost of synthesizing and applying nanoparticles at large scales may hinder their widespread adoption in environmental remediation (Qian *et al.,* 2020). Therefore, while nanotechnology offers great promise, its implementation must be carefully regulated to ensure that it does not introduce unintended consequences into the environment.

Recent advancements in nanotechnology have expanded its potential applications in the restoration of polluted soils. Researchers have explored the use of various nanoparticles, including metal nanoparticles, carbon-based nanomaterials, and hybrid systems, for effective soil detoxification. These materials have shown significant potential in removing both inorganic and

organic pollutants from soils, which are critical for restoring land quality and preventing further environmental damage. As research continues, the efficiency of nanoparticle-based remediation is expected to improve, with innovations focusing on enhancing the stability and reactivity of these materials (Rajput *et al.,* 2022).

1.2.2 Metal Oxide Nanoparticles for Heavy Metal Remediation

Nanotechnology plays a pivotal role in the remediation of contaminated soils. The use of nanoparticles in soil remediation is a highly promising field due to the unique properties of nanoparticles, including their large surface area, high reactivity, and ability to interact with contaminants in ways that bulk materials cannot. Nanoparticles can be engineered to target specific contaminants and offer significant advantages over traditional remediation techniques such as chemical extraction and bioremediation. These materials are not only capable of removing pollutants but can also immobilize them, preventing further contamination of the environment (Qian *et al.,* 2020). The ability of nanoparticles to penetrate soil and interact at the molecular level makes them an excellent tool for addressing environmental pollution, especially heavy metals.

Studies by Chauhan *et al.* (2024) have shown that doping MgO with transition metals such as cobalt (Co), copper (Cu), and zinc (Zn) significantly enhances its remediation capabilities. These doped nanoparticles exhibit improved reactivity and selectivity for different pollutants, making them even more effective in removing heavy metals from contaminated soils and water sources. The enhanced catalytic properties of metal-doped MgO nanoparticles allow for more efficient degradation of pollutants, providing an advanced solution for environmental cleanup. The

incorporation of transition metals into MgO nanoparticles is a promising approach that enhances their stability and performance in complex environmental conditions.

Nanoparticles such as MgO have shown significant promise in wastewater treatment applications, owing to their ability to adsorb and neutralize toxic substances. Perera *et al.* (2024) emphasized the versatility of MgO nanoadsorbents in treating various industrial effluents, particularly in the removal of heavy metals such as lead, mercury, and arsenic. MgO nanoparticles can be synthesized through both green and conventional methods, providing flexibility in their application depending on environmental and economic factors.

The interaction between metal oxide nanoparticles and pollutants follows mechanisms like adsorption, precipitation, and ion exchange. These mechanisms are integral to the efficiency of nanoparticle-based remediation systems. Adsorption is the process by which pollutants bind to the surface of nanoparticles, while precipitation involves the transformation of contaminants into insoluble forms that can be easily removed from the environment. Ion exchange allows for the replacement of harmful ions with less toxic ones, further enhancing the effectiveness of these nanomaterials (Wang *et al.,* 2020). The combination of these mechanisms in a single nanoparticle system maximizes the potential for successful environmental remediation.

Furthermore, studies by Ahmed *et al.* (2021) demonstrated the potential of MgO nanoparticles to modulate cellular oxidative repair mechanisms in plants, significantly reducing the uptake and translocation of toxic metals like arsenic. This ability to reduce metal toxicity in crops presents an additional advantage for MgO nanoparticles, which can be applied not only in soil remediation but also in agriculture to improve soil health and crop yield.

Fouda *et al.* (2021) further investigated the catalytic properties of MgO nanoparticles in wastewater treatment, showing their efficacy in degrading pollutants from the textile and tannery industries. The green synthesis of MgO nanoparticles using natural reagents enhances their environmental compatibility, making them an attractive option for sustainable remediation practices. These findings suggest that MgO-based nanomaterials could offer a versatile and effective solution for various environmental pollution problems, including soil contamination by heavy metals.

1.2.3 Biochar as a Remediation Agent

Fig 1.1: Biochar from Coconnut shells

Biochar is a carbon-rich material produced through the pyrolysis of organic substances, typically derived from biomass such as agricultural by-products, wood, and waste materials. Its properties—such as its high surface area, stability, and capacity for adsorbing contaminants—make it an effective tool for soil remediation (Ji *et al.,* 2022). The process of making biochar involves heating organic material in a low-oxygen environment, resulting in a substance that is chemically stable and thermally resistant, making it well-suited for long-term environmental

applications. Biochar is particularly effective in removing a range of pollutants, including heavy metals, toxic chemicals, and excess nutrients from contaminated soils.

When combined with metal oxide nanoparticles, biochar's effectiveness in soil remediation is enhanced due to the synergistic interactions between the materials. Biochar helps improve the surface area and reactivity of nanoparticles, contributing to heavy metal immobilization through mechanisms like adsorption, ion exchange, and chemical bonding (Gao *et al.,* 2022). By combining biochar with nanoparticles like magnesium oxide (MgO) and manganese oxide (MnO), a ternary nanocomposite is formed that can target and eliminate contaminants from the environment, offering an eco-friendly and cost-effective solution for soil cleanup.

Research has shown that biochar can significantly improve the performance of metal oxide nanoparticles by helping to retain the nanoparticles within the soil, thereby prolonging their contact with contaminants. The porous structure of biochar provides ample surface area for the adsorption of contaminants, while also serving as a matrix that prevents the nanoparticles from leaching away (Guo *et al.,* 2020). This combination increases the overall efficiency of contamination removal and ensures more stable immobilization of heavy metals, positioning this approach as a promising technique for sustainable environmental cleanup.

Furthermore, biochar can enhance the physical and chemical qualities of contaminated soils, such as raising soil pH, reducing acidity, and increasing nutrient availability. These changes can also support plant growth, making biochar a beneficial addition to agricultural environments affected by soil contamination. Its dual role in improving soil quality while removing pollutants makes biochar an excellent option for sustainable land management (Yang *et al.,* 2021).

Recent studies have also incorporated machine learning to predict how biochar amendments influence metal immobilization in soils, providing valuable insights into the efficiency of biochar-based remediation strategies (Sun *et al.,* 2022). These advancements allow for more precise and effective application of biochar in various environmental contexts, optimizing the success of soil remediation efforts.

1.2.4 *Ficus exasperata*

Ficus exasperata Vahl, commonly referred to as the sandpaper leaf, is a tropical plant prevalent across Africa, Asia, and South America. Traditionally employed in folk medicine to treat wounds, inflammation, and cardiovascular conditions, recent scientific studies have substantiated its medicinal properties, linking them to its rich phytochemical profile (Akinloye and Ugbaja, 2022).

Studies on the use of *Ficus exasperata* have revealed its diverse phytochemical composition, comprising flavonoids, tannins, alkaloids, saponins, phenols, and terpenoids. According to Mohammed et al. (2022a), gas chromatography-mass spectrometry (GC-MS) analysis of the ethyl acetate extract identified key compounds such as hexadecanoic acid, phytol, and linoleic acid. These bioactive compounds possess antioxidant and reducing properties, which are essential for stabilizing nanoparticle systems.

Further investigations by Mohammed et al. (2022b) into the chloroform extract of *Ficus exasperata* identified additional bioactive components, including stigmasterol, campesterol, and β-sitosterol. These phytochemicals not only exhibit pharmacological properties but also function as capping agents during nanoparticle synthesis, thereby enhancing stability and preventing particle agglomeration.

The reducing and stabilizing capabilities of *Ficus exasperata*, primarily attributed to its flavonoids and phenolic compounds, play a critical role in green synthesis. These compounds donate electrons to metal ions, facilitating their reduction into nanoparticles while simultaneously capping the newly formed particles. This dual functionality ensures the synthesis of stable, monodispersed nanoparticles with desirable physicochemical characteristics (Akinloye and Ugbaja, 2022).

Moreover, the antioxidant properties of *Ficus exasperata* further contribute to nanoparticle stability by preventing oxidative degradation. Mohammed et al. (2022a) reported that the plant's phytochemicals form a protective layer around nanoparticles, reducing surface energy and enhancing colloidal stability. This attribute makes *Ficus exasperata* an effective green solvent for synthesizing metal oxide-based nanocomposites, such as the MgO-MnO-Biochar system.

Studies on the use of *Ficus exasperata* in nanoparticle synthesis have demonstrated promising outcomes. Idowu et al. (2021) reported the biosynthesis of silver nanoparticles (AgNPs) using *Ficus exasperata* leaf extract, which exhibited significant larvicidal activity against *Anopheles gambiae*, a malaria vector. This finding underscores the plant's potential as a bio-reducing and stabilizing agent in green nanotechnology.

Similarly, Vazhacharickal and Krishnan (2018) employed *Ficus exasperata* latex extract to synthesize silver, copper, and zinc nanoparticles. The resulting nanoparticles displayed enhanced antibacterial activity, further supporting the plant's effectiveness in stabilizing nanoparticle systems.

The rich phytochemical profile and demonstrated nanoparticle-stabilizing properties of *Ficus exasperata* make it an ideal candidate for the green synthesis of MgO-MnO-Biochar ternary nanocomposites. The presence of phenolics, flavonoids, and terpenoids facilitates effective reduction, capping, and stabilization of nanoparticles, thereby enhancing their structural integrity and performance in potential environmental applications.

By utilizing *Ficus exasperata* extract as a green solvent, this study seeks to produce a stable, eco-friendly nanocomposite while mitigating the environmental and health risks associated with conventional synthesis methods. Insights from previous studies (Idowu *et al.,* 2021; Vazhacharickal and Krishnan, 2018) will guide the synthesis and characterization process, ensuring the development of high-quality ternary nanocomposites.

CHAPTER TWO

MATERIALS AND METHODS

2.1 Materials

2.1.1 Reagent

- *Ficus exasperata* leaf extract
- Magnesium chloride hexahydrate ($MgCl_2.6H_2O$)
- Manganese chloride tetrahydrate ($MnCl_2.4H_2O$)
- Distilled water
- Ethanol
- Sodium hyroxide (NaOH)

2.1.2 Apparatus

- 200mL Beakers
- Stirring rods
- 150mL Conical flasks
- Measuring cylinder
- Filter Paper
- Crucible
- 1L Volumetric Flask
- Wash bottle
- Mortar

- Pestle
- Beakers
- Graduated cylinder
- Spatula
- Filter paper
- Round-bottom flask

2.1.3 Equipment

- Weighing balance
- Hot plate
- Magnetic stirrer
- pH Meter
- Thermometer
- Pyrolysis Reactor
- Oven
- Muffle Furnace

2.2 Methods

2.2.1 Preparation of Solution

2.2.1.1 Preparation of Precursors

Magnesium and manganese salts were prepared as precursors for the nanoparticle synthesis by dissolving accurately weighed amounts of magnesium chloride hexahydrate ($MgCl_2 \cdot 6H_2O$) and manganese chloride tetrahydrate ($MnCl_2 \cdot 4H_2O$) in distilled water. Specifically, 6.1g of

$MgCl_2 \cdot 6H_2O$ was dissolved in approximately 100 mL of distilled water in a 250mL beaker. The mixture was stirred until complete dissolution was achieved, after which 50mL was added to obtain a 0.1M magnesium chloride solution. Similarly, 2.9g of $MnCl_2 \cdot 4H_2O$ was dissolved in about 100mL of distilled water in a separate 250mL beaker. The solution was stirred thoroughly until the salt dissolved completely, then topped up with 50mL distilled water to yield a 0.2M manganese chloride solution. Both solutions were prepared in a 2:1 molar ratio, stored in labeled containers, and handled with care due to the potential irritant nature of the chloride salts.

2.2.1.2 Preparation of Alkali

Sodium hydroxide (NaOH) solution with a concentration of 1M was prepared by dissolving an accurately weighed amount of sodium hydroxide pellets in distilled water. Specifically, 40.00 g of NaOH, corresponding to its molar mass, was measured using an analytical balance and transferred into a clean 500mL beaker containing approximately 300 mL of distilled water. The mixture was stirred continuously using a glass rod until the pellets dissolved completely, generating a clear, homogeneous solution. The resulting solution was then transferred into a 1L volumetric flask, and distilled water was added up to the 1L mark to achieve the desired 1M concentration. The solution was stored in a tightly sealed, labeled container and handled with care due to the caustic nature of sodium hydroxide.

2.2.2 Preparation of *Ficus exasperata*

The extraction of *Ficus exasperata* leaves was carried out using the decoction method. Fresh leaves of *Ficus exasperata* were collected, washed thoroughly with distilled water to remove surface impurities, and cut into smaller pieces. The prepared leaves were transferred into a stainless steel pot, and distilled water was added in a 1:10 (w/v) ratio. The mixture was heated to

60°C and maintained at this temperature for 1 hour, ensuring efficient extraction of water-soluble phytochemicals while preserving heat-sensitive compounds.

After the heating process, the mixture was allowed to cool to room temperature and then filtered using Whatman No. 1 filter paper to separate the plant residue from the liquid extract. The filtrate was collected in a clean, airtight container and stored at 4°C for subsequent analyses. This controlled decoction process provided an effective means of extracting the bioactive constituents of *Ficus exasperata* while minimizing potential degradation due to excessive heat.

2.2.3 Preparation of Biochar

The preparation of biochar from coconut shells was carried out through a pyrolysis process. Fresh coconut shells were collected, washed thoroughly with distilled water to remove dirt, fibers, and residual organic matter, and then air-dried for 5–7 days to ensure complete moisture removal. The dried shells were subsequently crushed into smaller pieces to increase the surface area for efficient carbonization.

The crushed coconut shells were placed in a stainless steel reactor and heated to 500°C under limited oxygen conditions to prevent combustion. The temperature was gradually increased at a rate of 10°C per minute until it reached 500°C, and this temperature was maintained for 3 hours to ensure complete pyrolysis. During this process, the lignocellulosic components of the shells underwent thermal decomposition, releasing volatile gases while leaving behind a carbon-rich biochar.

After pyrolysis, the reactor was allowed to cool to room temperature. The resulting biochar was collected, ground to a uniform particle size, and sieved through a 2mm mesh to obtain a

consistent material. The biochar was then stored in airtight containers to prevent moisture absorption and was subsequently characterized for its surface area, pore structure, and elemental composition.

2.3 Synthesis of Ternary Nanoparticle

2.3.1 Synthesis of the Binary Nanoparticle System

The synthesis of binary nanoparticles was carried out using the pre-prepared 0.2 M magnesium chloride ($MgCl_2$) and 0.1M manganese chloride ($MnCl_2$) solutions in a 2:1 molar ratio. The solutions were combined in a beaker under continuous stirring at room temperature to ensure homogeneity. The mixture was then heated to 60°C and 15 mL of *Ficus exasperata* leaf extract was added (which corresponds to 5% of the solution) and stirred for 1 hour to facilitate the interaction of the metal ions. A 1M sodium hydroxide (NaOH) solution was added dropwise to the mixture until the pH reached 10–11, inducing the co-precipitation of magnesium-manganese hydroxide n anoparticles. The precipitate formed was stirred continuously for another 2 hours maintaining the temperature at 60^{o}C to promote uniform particle growth.

The resultant precipitate was separated by centrifugation at 10,000 rpm for 5 minutes, washed repeatedly with distilled water to remove impurities, followed by a final rinse with ethanol to aid in drying. The washed sample was dried in an oven at 105°C for 4 hours and stored in an airtight container for further conversion to their ternary system.

2.3.2 Synthesis of the Ternary Nanoparticle System

The incorporation of the synthesized binary nanoparticles with biochar was carried out to enhance their surface properties and potential applications to create the ternary nanoparticle system. The dried biochar, prepared from coconut shells, was ground to a fine powder and sieved

through a 2mm mesh to ensure uniform particle size. A calculated amount of the biochar was dispersed in distilled water under continuous stirring to create a homogeneous slurry.

The binary nanoparticles were gradually added to the biochar slurry in a 10:1 mass ratio (10g of biochar to 1g of nanoparticles) while maintaining constant stirring at room temperature. The mixture was stirred for 2 hours to ensure even distribution and interaction between the nanoparticles and the biochar surface. The incorporated material was subsequently filtered, washed with distilled water to remove unbound particles, and dried in an oven at 80°C for 6 hours.

After drying, the biochar-incorporated nanoparticles were calcined at 600°C for 4 hours to enhance their structural integrity and improve surface properties. The calcined material was allowed to cool to room temperature and stored in an airtight container for further characterization and application in experimental studies.

2.4 Characterization of the Ternary Nanoparticle System

The synthesized nanoparticles were characterized using Fourier Transform Infrared Spectroscopy (FTIR) Model Cary 630 by NBY Agilent Technologies, X-ray Diffraction (XRD) Model JSM-7600F, Brunauer–Emmett–Teller (BET) surface area analysis, and Schottky Field Emission Scanning Electron Microscopy with Energy Dispersive X-ray Spectroscopy (SEM-EDX) to assess their structural, morphological, textural, and elemental properties.

FTIR analysis was conducted to identify the functional groups present in the activated nanoparticle samples, providing insights into the interaction between the alkali-treated

nanoparticles and any other compounds present. This facilitated an understanding of the bonding mechanisms and potential chemical changes occurring during the activation process.

XRD analysis was employed to determine the crystalline structure and phase composition of the activated nanoparticles, enabling the evaluation of structural changes that might have resulted from the thermal activation process at different temperatures. The XRD results offered insight into the dispersion of mineral phases and possible modifications induced by the activation.

BET surface area analysis was performed to determine the specific surface area, pore size, and pore volume of the nanoparticle samples. This analysis provided essential information regarding the textural properties of the materials, which are critical in applications such as adsorption and catalysis. The results allowed for the correlation of surface characteristics with the synthesis and activation conditions applied.

SEM was used to investigate the surface morphology of the nanoparticle samples, revealing information about particle size, shape, and distribution. Additionally, EDX provided elemental analysis to confirm the presence of elements such as magnesium, manganese, and carbon, ensuring that the calcination process had not caused significant changes in the elemental composition of the nanoparticles.

CHAPTER THREE

RESULTS AND DISCUSSION

3.1 Results

The MgO-MnO-Biochar nanocomposite and the MgO-MnO nanoparticle system underwent detailed characterization using Fourier Transform Infrared Spectroscopy (FTIR), Energy Dispersive X-ray Spectroscopy (EDX), X-ray Diffraction (XRD), and Brunauer-Emmett-Teller (BET) surface area analysis to evaluate structural, elemental, and textural modifications resulting from synthesis and thermal treatment. Table 3.1 presents the FTIR spectra for the MgO-MnO-Biochar nanocomposite and MgO-MnO nanoparticle system, highlighting changes in functional groups and structural transformations induced during composite formation. Table 3.2 provides the EDX analysis, detailing the elemental compositions of both the MgO-MnO-Biochar nanocomposite and the MgO-MnO nanoparticle system, showing variations in elemental concentrations attributed to the synthesis process. The XRD patterns and phase compositions of the MgO-MnO-Biochar nanocomposite and MgO-MnO nanoparticle system are presented in Table 3.3, identifying crystalline structures and phase transitions associated with composite formation and thermal conditions. Table 3.4 compares the BET surface area, pore volume, and pore diameter for the MgO-MnO-Biochar nanocomposite and the MgO-MnO nanoparticle system, illustrating textural differences and the impact of synthesis conditions on porosity and surface area. Each characterization technique offers a comprehensive comparison, demonstrating how the synthesis process influences the chemical, structural, and surface properties of the MgO-MnO-Biochar nanocomposite and the MgO-MnO nanoparticle system.

Table 3.1: Results for the FT-IR Analysis

Sample	Band (cm^{-1})	Assignment
MgO-MnO-Biochar Nanocomposite	3951.1, 3641.1, 3790.2	O–H stretching (hydroxyl groups)
	3398.2	H–O–H bending (adsorbed water)
	2907.3	C–H stretching (aliphatic compounds)
	2110.3	CO_2 adsorption
	1611.8	C=C stretching (aromatic rings)
	1401.6	C–O stretching (phenols, carboxyls)
	1030.2	Si–O–Si or C–O stretching
	946.3, 864.7	Metal-O bonds (Mg–O, Mn–O)
MgO-MnO Nanoparticle	2102.2	CO_2 adsorption
	1598.5	C=C stretching (aromatic rings)
	1372.3	C–O stretching (phenols, carboxyls)
	1004.4	Si–O–Si or C–O stretching

The Fourier Transform Infrared (FT-IR) analysis of the MgO-MnO-Biochar nanocomposite and the MgO-MnO nanoparticle system revealed distinct functional group vibrations, providing insights into their structural composition. The MgO-MnO-Biochar nanocomposite exhibited a

broad peak at 3951.1, 3641.1, and 3790.2 cm^{-1}, corresponding to O–H stretching vibrations associated with hydroxyl groups. These bands indicate the presence of surface-bound hydroxyl groups, which play a crucial role in enhancing the nanocomposite's adsorption capacity and surface reactivity. Additionally, a peak at 3398.2 cm^{-1} was attributed to H–O–H bending, suggesting the presence of adsorbed water molecules on the nanocomposite surface.

The presence of C–H stretching vibrations from aliphatic compounds was confirmed by the band at 2907.3 cm^{-1}, while a prominent peak at 2110.3 cm^{-1} indicated CO_2 adsorption, reflecting the surface's ability to interact with gaseous molecules. The peak observed at 1611.8 cm^{-1} was assigned to C=C stretching, characteristic of aromatic rings, signifying the structural contribution of biochar. Furthermore, the band at 1401.6 cm^{-1} corresponded to C–O stretching, often associated with phenolic and carboxyl groups, suggesting functionalized biochar within the nanocomposite. The Si–O–Si or C–O stretching vibrations, observed at 1030.2 cm^{-1}, further validated the biochar's incorporation. The bands at 946.3 and 864.7 cm^{-1} were linked to metal-oxygen (Mg–O and Mn–O) bonds, confirming the successful synthesis of the ternary nanocomposite.

In contrast, the MgO-MnO nanoparticle system displayed fewer functional group vibrations, reflecting its simpler structure compared to the biochar-incorporated composite. A peak at 2102.2 cm^{-1} indicated CO_2 adsorption, suggesting surface interaction sites. The C=C stretching vibration at 1598.5 cm^{-1}, characteristic of aromatic rings, was less prominent compared to the nanocomposite, reflecting the absence of biochar's aromatic framework. Similarly, the C–O stretching at 1372.3 cm^{-1}, associated with phenolic and carboxyl groups, appeared with lower

intensity, indicating reduced surface functionalization. The presence of Si–O–Si or C–O stretching at 1004.4 cm^{-1} further confirmed the structural integrity of the nanoparticles.

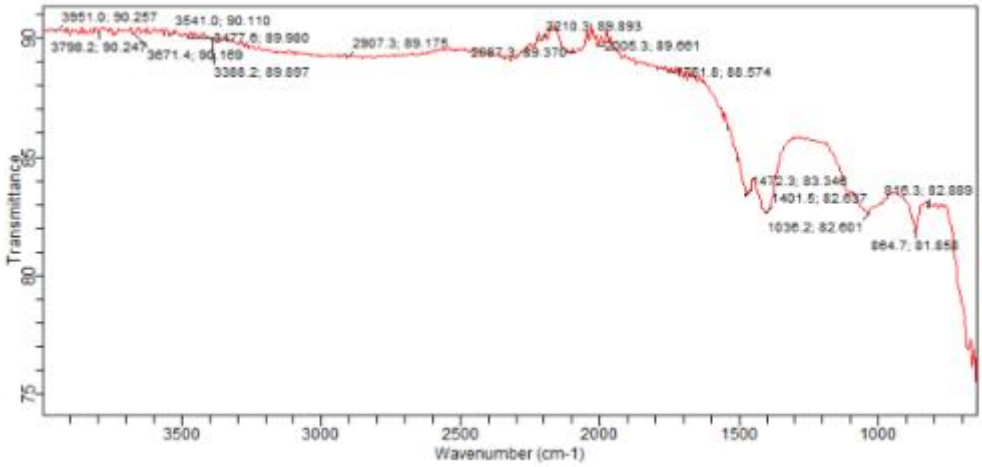

Fig 3.1: FTIR Spectra of MgO-MnO-Biochar Nanocomposite

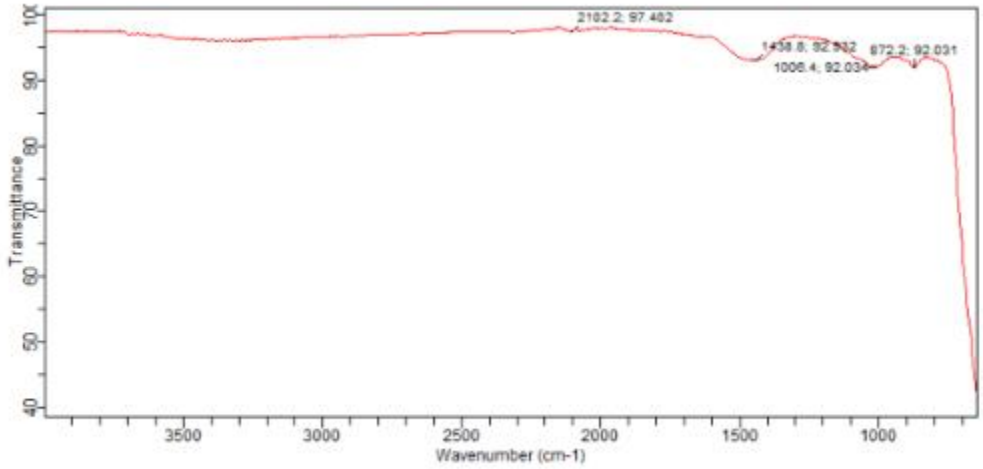

Fig 3.2: FTIR Spectra of MgO-MnO Nanoparticle System

Table 3.2: Results for the EDX for the samples

Element Name	MgO-MnO-Biochar Nanocomposite Wt(%)	MgO-MnO nanoparticle system Wt(%)
Carbon (C)	48.72	-
Manganese (Mn)	24.47	61.62
Magnesium (Mg)	11.34	32.24
Potassium (K)	8.00	-
Calcium (Ca)	2.80	0.81
Chlorine (Cl)	1.53	2.30
Silicon (Si)	0.90	0.35
Potassium (P)	0.86	0.08
Sodium (Na)	0.83	2.19
Aluminium (Al)	0.34	0.40
Sulphur (S)	0.20	-

The Energy Dispersive X-ray

Spectroscopy (EDX) analysis provided detailed insights into the elemental composition of the MgO-MnO-Biochar nanocomposite and the MgO-MnO nanoparticle system. The results revealed significant differences in elemental distribution, reflecting the influence of biochar incorporation and synthesis conditions on the final material composition.

The MgO-MnO-Biochar nanocomposite exhibited a high carbon content of 48.72 wt%, attributed to the biochar component derived from biomass. This substantial carbon presence not only enhances the surface area but also provides functional groups that facilitate adsorption processes. In contrast, the MgO-MnO nanoparticle system lacked carbon, indicating the absence of biochar in its synthesis pathway.

Manganese (Mn) and magnesium (Mg) were prominent elements in both systems, though their concentrations varied significantly. In the MgO-MnO nanoparticle system, manganese accounted for 61.62 wt%, while magnesium constituted 32.24 wt%. This higher concentration suggests a more concentrated formation of metal oxides in the nanoparticle system. Conversely, the MgO-MnO-Biochar nanocomposite contained 24.47 wt% manganese and 11.34 wt% magnesium, reflecting the dilution effect caused by biochar integration.

Notably, the MgO-MnO-Biochar nanocomposite contained 8.00 wt% potassium (K), an element absent in the nanoparticle system. The presence of potassium, along with 2.80 wt% calcium (Ca), 1.53 wt% chlorine (Cl), and 0.90 wt% silicon (Si), suggests that the biochar retained essential minerals from the biomass source. In comparison, the MgO-MnO nanoparticle system exhibited lower levels of these elements, with calcium at 0.81 wt%, chlorine at 2.30 wt%, and silicon at 0.35 wt%.

Furthermore, the MgO-MnO-Biochar nanocomposite contained trace amounts of phosphorus (0.86 wt%), sodium (0.83 wt%), aluminum (0.34 wt%), and sulfur (0.20 wt%). In contrast, the nanoparticle system showed reduced concentrations of phosphorus (0.08 wt%), sodium (2.19 wt%), and aluminum (0.40 wt%), while sulfur was completely absent.

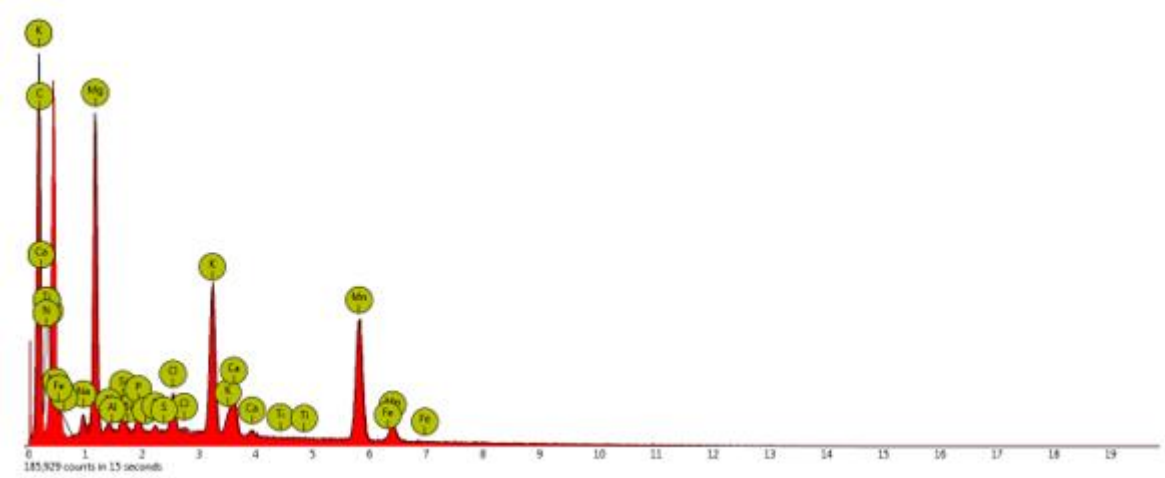

Fig 3.3: EDX Profile of MGO-MNO-BIOCHAR NANOCOMPOSITE

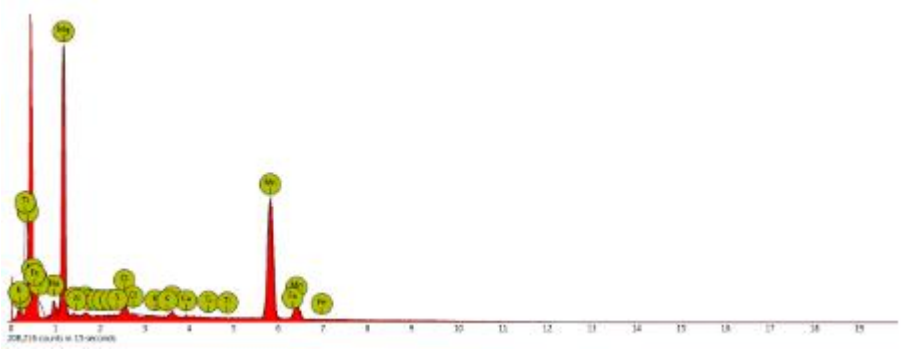

Fig 3.4: EDX Profile of MgO-MnO Nanoparticle System

The SEM images reveal distinct morphological differences between the two samples. The first set of images exhibits a highly porous and heterogeneous structure with well-dispersed particles

and a rough texture. The presence of fibrous and irregularly shaped structures suggests a composite material with embedded nanoparticles, which could enhance surface area and provide active sites for adsorption or catalytic processes.

In contrast, the second set of images displays a more compact and aggregated morphology with larger, irregularly shaped particles and a denser surface. The reduced porosity and smoother texture indicate possible sintering or particle fusion, which could influence the material's surface reactivity and interaction with external substances. The differences in these microstructural features suggest variations in synthesis methods or material composition, which could impact their performance in specific applications such as adsorption, catalysis, or environmental remediation.

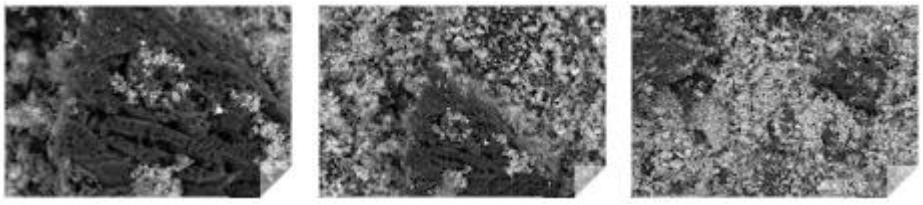

Fig. 3.5: SEM Images for MgO-MnO-Biochar Nanocomposite

Fig. 3.6: SEM Images for MgO-MnO Nanoparticle System

Table 3.3: Results of the XRD for the both samples

Mineral Name	Chemical Formula	% in MgO-MnO-Biochar Nanocomposite	% in MgO-MnO Nanoparticle System
Lindergerbite	$MgFBO_3$	26.88	59.00
Flagstaffite	SiO_2	52.40	-
Jacobsite	$MnFe_2O_4$	10.92	16.00
Graphite	C	1.84	-
Cryoptohalite	K_3AlF_6	7.96	-
Periclase	MgO	-	13.00
Quartz	SiO_2	-	11.20

The X-ray diffraction (XRD) analysis revealed significant variations in the mineralogical composition between the MgO-MnO-Biochar nanocomposite and the MgO-MnO nanoparticle system. Lindergerbite ($MgFBO_3$) was detected in both samples, with a higher concentration in the MgO-MnO nanoparticle system (59.00%) compared to the MgO-MnO-Biochar

nanocomposite (26.88%). This higher percentage suggests that the absence of biochar during synthesis enhances the formation of Lindergerbite, likely due to fewer competing interactions during crystallization.

Flagstaffite (SiO_2) was the dominant phase in the MgO-MnO-Biochar nanocomposite, comprising 52.40% of the mineral composition, while it was absent in the MgO-MnO nanoparticle system. The presence of biochar likely facilitated the incorporation of silica-based compounds, promoting the formation of Flagstaffite during composite synthesis.

Jacobsite ($MnFe_2O_4$), a spinel ferrite, was present in both samples, with 10.92% in the nanocomposite and 16.00% in the nanoparticle system. The higher concentration in the MgO-MnO nanoparticle system suggests that the biochar component in the composite may have inhibited the crystallization of Jacobsite, possibly by altering the redox conditions during synthesis.

Graphite (C), a key component associated with the biochar matrix, was present exclusively in the MgO-MnO-Biochar nanocomposite at 1.84%. Its absence in the MgO-MnO nanoparticle system confirms that the carbonaceous material derived from biochar was effectively incorporated during composite formation.

Cryoptohalite (K_3AlF_6) was detected only in the MgO-MnO-Biochar nanocomposite at 7.96%. This mineral's formation is likely facilitated by the potassium and aluminum content introduced by the biochar matrix, indicating the complex role of biochar in promoting specific mineral phases.

Periclase (MgO) appeared exclusively in the MgO-MnO nanoparticle system at 13.00%. The absence of biochar likely provided favorable conditions for the formation of pure magnesium oxide, as biochar could hinder the direct crystallization of MgO during composite synthesis.

Quartz (SiO_2), another silica-based mineral, was found only in the MgO-MnO nanoparticle system at 11.20%. The absence of biochar likely promoted the crystallization of quartz, as the carbonaceous matrix in the nanocomposite might have restricted the availability of free silica for quartz formation.

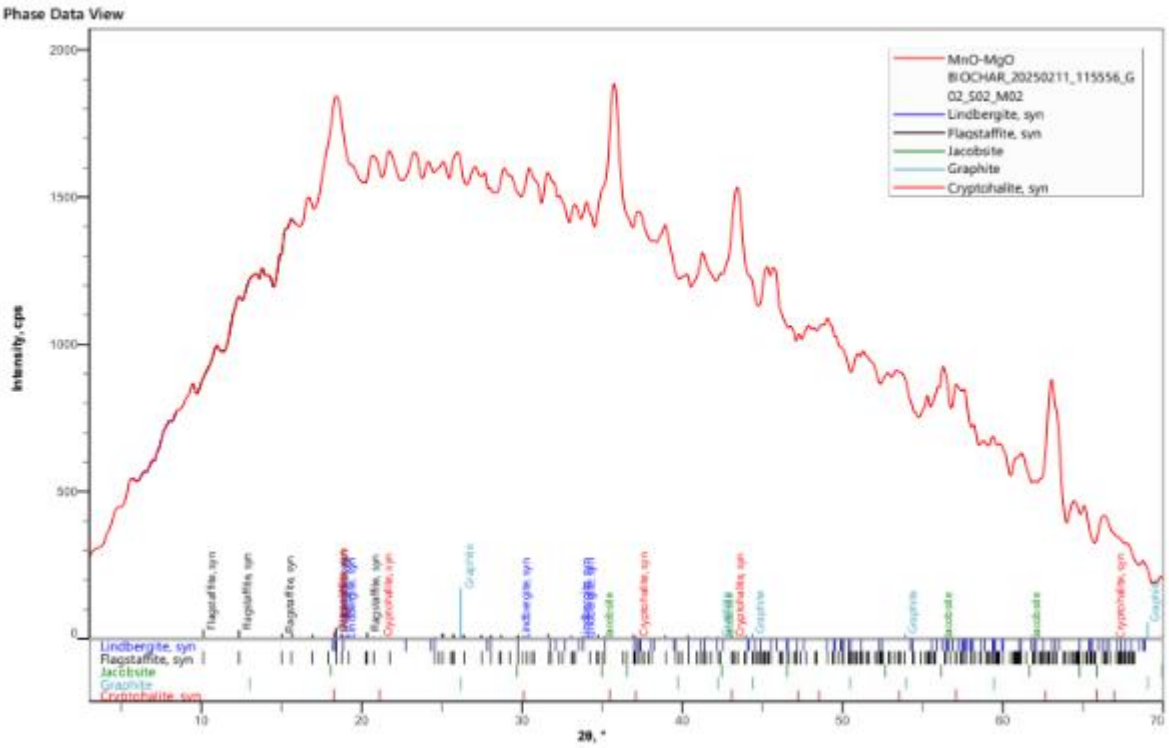

Fig. 3.7: XRD Pattern for MgO-MnO-Biochar Nanocomposite

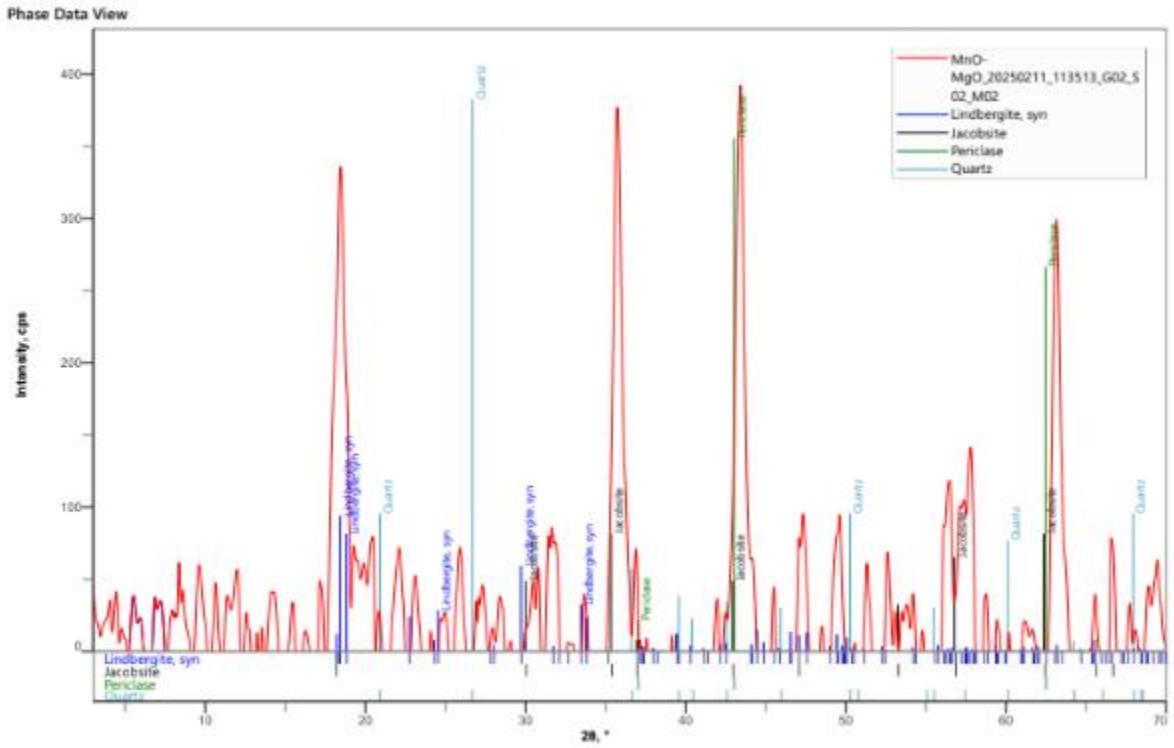

Fig. 3.8: XRD Pattern for MnO-MnO Nanoparticle System

Table 3.4: Results of the BET for the samples

Characterization	**MgO-MnO-Biochar Nanocomposite**	**MgO-MnO Nanoparticle System**
Surface Area by BET(m^2/g)	216.400	282.000
Surface area by t-plot (m^2/g)	216.400	282.000
Surface area by BJH adsorption (m^2/g)	265.400	354.200

Pore Volume (cm^3/g	0.128	0.173
Pore Diameter (nm)	2.129	2.132

The BET analysis in Table 3.4 provides insight into the surface area, pore volume, and pore diameter of the MgO-MnO-Biochar nanocomposite compared to the MgO-MnO nanoparticle system. The MgO-MnO nanoparticle system exhibits a higher BET surface area (282.000 m^2/g) compared to the MgO-MnO-Biochar nanocomposite (216.400 m^2/g). This increased surface area in the nanoparticle system suggests more active sites for adsorption, likely due to the absence of biochar, which can partially occupy available surface sites.

Similarly, the BJH adsorption surface area, which focuses on mesopores, is higher for the MgO-MnO nanoparticle system (354.200 m^2/g) compared to the MgO-MnO-Biochar nanocomposite (265.400 m^2/g). This indicates that the addition of biochar slightly reduces mesoporous surface availability, possibly due to biochar particles blocking some pores.

The pore volume follows the same trend, with the MgO-MnO nanoparticle system having a higher pore volume (0.173 cm^3/g) than the MgO-MnO-Biochar nanocomposite (0.128 cm^3/g). This further supports the idea that biochar incorporation reduces available pore space.

However, the pore diameters remain relatively similar between the two systems, with the MgO-MnO-Biochar nanocomposite showing an average diameter of 2.129 nm and the MgO-MnO nanoparticle system showing 2.132 nm. This suggests that while the biochar reduces surface area and pore volume, it does not significantly alter the pore size distribution.

Fig. 3.9: BET Multiplot for MgO-MnO-Biochar Nanocomposite

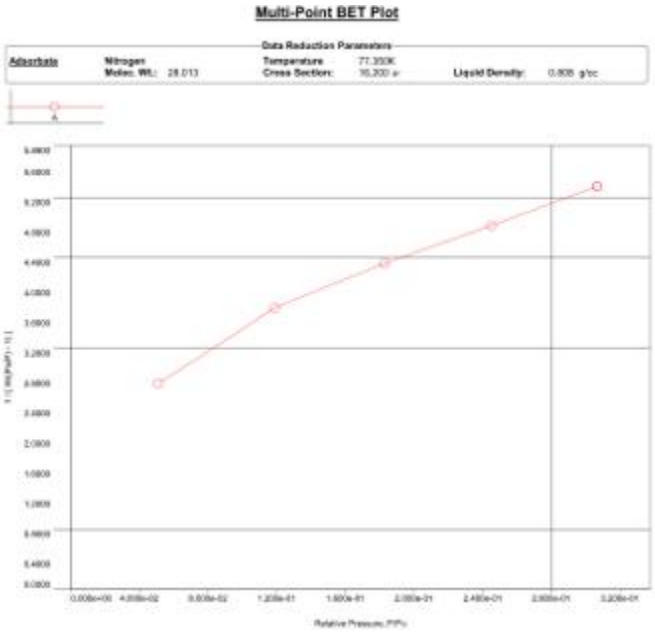

Fig. 3.10: BET Multiplot for MgO-MnO Nanoparticle System

3.2 Conclusion

This study successfully synthesized and characterized MgO-MnO-Biochar nanocomposite and MgO-MnO nanoparticle systems, highlighting their structural, morphological, and surface properties. FT-IR analysis confirmed the presence of functional groups that contribute to the nanocomposite's enhanced adsorption capacity, with biochar incorporation introducing additional hydroxyl and carbonyl functionalities. EDX analysis demonstrated a significant difference in elemental composition, with the nanocomposite exhibiting higher carbon content and trace elements derived from biochar, while the nanoparticle system had a more concentrated presence of metal oxides. XRD results revealed the presence of distinct mineral phases, with biochar incorporation influencing crystal formation, leading to the presence of Flagstaffite and Graphite in the nanocomposite while promoting Periclase and Quartz formation in the nanoparticle system. BET analysis indicated a higher surface area and pore volume for the nanoparticle system, suggesting greater availability of active sites, though the nanocomposite retained a favorable porous structure. Finally, The SEM revealed distinct morphological differences, with the first sample showing a porous, heterogeneous structure ideal for adsorption, while the second displayed a compact, aggregated morphology with reduced porosity but greater stability. These variations highlight the influence of synthesis conditions on material performance. These findings underscore the potential application of MgO-MnO-Biochar nanocomposites in environmental remediation, particularly in heavy metal adsorption, due to their enhanced surface functionality and structural diversity. Future studies should explore the composite's adsorption kinetics and long-term stability to optimize its practical application in wastewater treatment and soil remediation.

REFERENCES

Ahmed, T., Noman, M., Manzoor, N., Shahid, M., Hussaini, K.M., Rizwan, M., Ali, S., Maqsood, A. and Li, B., 2021. Green magnesium oxide nanoparticles-based modulation of cellular oxidative repair mechanisms to reduce arsenic uptake and translocation in rice (Oryza sativa L.) plants. Environmental pollution, 288, p.117785.

Akinloye, O. and Ugbaja, R. (2022) 'Phytochemical composition and medicinal potential of *Ficus exasperata* Vahl.', *Journal of Medicinal Plants Research*, 16(5), pp. 112–123.

Aparicio, J.D., Raimondo, E.E., Saez, J.M., Costa-Gutierrez, S.B., Alvarez, A., Benimeli, C.S. and Polti, M.A., 2022. The current approach to soil remediation: a review of physicochemical and biological technologies, and the potential of their strategic combination. Journal of Environmental Chemical Engineering, 10(2), p.107141.

Bakshi, M. and Abhilash, P.C., 2020. Nanotechnology for soil remediation: Revitalizing the tarnished resource. In Nano-materials as photocatalysts for degradation of environmental pollutants (pp. 345-370). Elsevier.

Bharti, R. and Sharma, R., 2022. Effect of heavy metals: An overview. Materials Today: Proceedings, 51, pp.880-885.

Chauhan, D., Kumar, R., Thakur, N. and Kumar, K., 2024. Exploring transition metal (Co, Cu, and Zn) doped magnesium oxide nanoparticles for their environmental remediation potential. Materials Science and Engineering: B, 302, p.117256.

Davidson, C.M., Duncan, A.L., Littlejohn, D., Ure, A.M. and Garden, L.M., 1998. A critical evaluation of the three-stage BCR sequential extraction procedure to assess the potential mobility and toxicity of heavy metals in industrially-contaminated land. Analytica Chimica Acta, 363(1), pp.45-55.

Ekrami, E., Pouresmaieli, M., sadat Hashemiyoon, E., Noorbakhsh, N. and Mahmoudifard, M., 2022. Nanotechnology: A sustainable solution for heavy metals remediation. Environmental Nanotechnology, Monitoring & Management, 18, p.100718.

Faizan, M., Bhat, J.A., El-Serehy, H.A., Moustakas, M. and Ahmad, P., 2022. Magnesium oxide nanoparticles (MgO-NPs) alleviate arsenic toxicity in soybean by modulating photosynthetic function, nutrient uptake and antioxidant potential. Metals, 12(12), p.2030.

Fouda, A., Hassan, S.E.D., Abdel-Rahman, M.A., Farag, M.M., Shehal-deen, A., Mohamed, A.A., Alsharif, S.M., Saied, E., Moghanim, S.A. and Azab, M.S., 2021. Catalytic degradation of wastewater from the textile and tannery industries by green synthesized hematite (α-Fe2O3) and magnesium oxide (MgO) nanoparticles. Current Research in Biotechnology, 3, pp.29-41.

Ganie, A.S., Bano, S., Khan, N., Sultana, S., Rehman, Z., Rahman, M.M., Sabir, S., Coulon, F. and Khan, M.Z., 2021. Nanoremediation technologies for sustainable remediation of contaminated environments: Recent advances and challenges. Chemosphere, 275, p.130065.

Gao, Y., Wu, P., Jeyakumar, P., Bolan, N., Wang, H., Gao, B., Wang, S. and Wang, B., 2022. Biochar as a potential strategy for remediation of contaminated mining soils: Mechanisms, applications, and future perspectives. Journal of environmental management, 313, p.114973.

Guo, M., Song, W. and Tian, J., 2020. Biochar-facilitated soil remediation: mechanisms and efficacy variations. Frontiers in Environmental Science, 8, p.521512.

HELAL, M.I., KHATER, H.A. and MARZOOG, A., 2016. Application of nanotechnology in remediation of heavy metals polluted soils. Journal of Arid Land Studies, 26(3), pp.129-137.

Idowu, A.O., Adewumi, A., Olaleye, M.T. and Olaniran, O.I. (2021) 'Green synthesis of silver nanoparticles using *Ficus exasperata* leaf extract and evaluation of their larvicidal activity against *Anopheles gambiae*', *Environmental Nanotechnology, Monitoring & Management*, 15, p. 100430.

Ji, M., Wang, X., Usman, M., Liu, F., Dan, Y., Zhou, L., Campanaro, S., Luo, G. and Sang, W., 2022. Effects of different feedstocks-based biochar on soil remediation: A review. Environmental Pollution, 294, p.118655.

Kristanti, R.A., Liong, R.M.Y. and Hadibarata, T., 2021. Soil remediation applications of nanotechnology. Tropical Aquatic and Soil Pollution, 1(1), pp.35-45.

Long, Z., Huang, Y., Zhang, W., Shi, Z., Yu, D., Chen, Y., Liu, C. and Wang, R., 2021. Effect of different industrial activities on soil heavy metal pollution, ecological risk, and health risk. Environmental Monitoring and Assessment, 193, pp.1-12.

Mohammed, A., Adeyemi, S.O., Balogun, F. and Yusuf, M. (2022a) 'GC-MS analysis of the ethyl acetate extract of *Ficus exasperata* leaves and its antioxidant properties', *Journal of Phytochemistry and Pharmacology*, 11(3), pp. 205–214.

Mohammed, A., Yusuf, M., Balogun, F. and Adeyemi, S.O. (2022b) 'Bioactive compounds from the chloroform extract of *Ficus exasperata* leaves and their role in nanoparticle synthesis', *International Journal of Green Nanotechnology*, 9(2), pp. 87–96.

Nemati, K., Bakar, N.K.A., Abas, M.R. and Sobhanzadeh, E., 2011. Speciation of heavy metals by modified BCR sequential extraction procedure in different depths of sediments from Sungai Buloh, Selangor, Malaysia. Journal of hazardous materials, 192(1), pp.402-410.

Okuo, J.M., Jacob, J.N., IE, U., Ogbeide, O.K., Imafidon, M.I. and Aghedo, O.N., 2022. Effects of Blighia sapida derived Biochar Amendment on Mobility and Bioavailability of Heavy Metals in Lead-Acid Battery Contaminated Soil. ChemSearch Journal, 13(1), pp.45-56.

Perera, H.C.S., Gurunanthanan, V., Singh, A., Mantilaka, M.M.M.G.P.G., Das, G. and Arya, S., 2024. Magnesium oxide (MgO) nanoadsorbents in wastewater treatment: A comprehensive review. Journal of Magnesium and Alloys.

Qian, Y., Qin, C., Chen, M. and Lin, S., 2020. Nanotechnology in soil remediation− applications vs. implications. Ecotoxicology and Environmental Safety, 201, p.110815.

Qian, Y., Qin, C., Chen, M. and Lin, S., 2020. Nanotechnology in soil remediation− applications vs. implications. Ecotoxicology and Environmental Safety, 201, p.110815.

Rajput, V.D., Minkina, T., Upadhyay, S.K., Kumari, A., Ranjan, A., Mandzhieva, S., Sushkova, S., Singh, R.K. and Verma, K.K., 2022. Nanotechnology in the restoration of polluted soil. Nanomaterials, 12(5), p.769.

Sun, Y., Zhang, Y., Lu, L., Wu, Y., Zhang, Y., Kamran, M.A. and Chen, B., 2022. The application of machine learning methods for prediction of metal immobilization remediation by biochar amendment in soil. Science of the Total Environment, 829, p.154668.

Sungur, A., Soylak, M. and Ozcan, H., 2014. Investigation of heavy metal mobility and availability by the BCR sequential extraction procedure: relationship between soil properties and heavy metals availability. Chemical Speciation & Bioavailability, 26(4), pp.219-230.

Susaimanickam, A., Selvaraj, D. and Manickam, P., 2024. Nanoparticle-based bioremediation of organic and inorganic substances from water bodies. In Bioremediation of Emerging Contaminants in Water. Volume 2 (pp. 135-162). American Chemical Society.

ur Rehman, Z., Junaid, M.F., Ijaz, N., Khalid, U. and Ijaz, Z., 2023. Remediation methods of heavy metal contaminated soils from environmental and geotechnical standpoints. Science of The Total Environment, 867, p.161468.

Vazhacharickal, P.J. and Krishnan, A. (2018) 'Green synthesis of silver, copper, and zinc nanoparticles using *Ficus exasperata* latex extract and evaluation of their antibacterial activity', *Journal of Nanomaterials and Biostructures*, 13(2), pp. 345–353.

Wang, R., Lou, J., Fang, J., Cai, J., Hu, Z. and Sun, P., 2020. Effects of heavy metals and metal (oxide) nanoparticles on enhanced biological phosphorus removal. Reviews in Chemical Engineering, 36(8), pp.947-970.

Wang, Z., Luo, P., Zha, X., Xu, C., Kang, S., Zhou, M., Nover, D. and Wang, Y., 2022. Overview assessment of risk evaluation and treatment technologies for heavy metal pollution of water and soil. Journal of Cleaner Production, 379, p.134043.

Wuana, R.A. and Okieimen, F.E., 2011. Heavy metals in contaminated soils: a review of sources, chemistry, risks and best available strategies for remediation. International Scholarly Research Notices, 2011(1), p.402647.

Xiang, M., Li, Y., Yang, J., Lei, K., Li, Y., Li, F., Zheng, D., Fang, X. and Cao, Y., 2021. Heavy metal contamination risk assessment and correlation analysis of heavy metal contents in soil and crops. Environmental Pollution, 278, p.116911.

Yadav, K.K., Cabral-Pinto, M.M., Gacem, A., Fallatah, A.M., Ravindran, B., Rezania, S., Algethami, J.S., Eltayeb, L.B., Abbas, M., Al-shareef, T.H. and Vinayak, V., 2024. Recent advances in the application of nanoparticle-based strategies for water remediation as a novel clean technology–A comprehensive review. Materials Today Chemistry, 40, p.102226.

Yang, Y., Ye, S., Zhang, C., Zeng, G., Tan, X., Song, B., Zhang, P., Yang, H., Li, M. and Chen, Q., 2021. Application of biochar for the remediation of polluted sediments. Journal of Hazardous Materials, 404, p.124052.

Yuan, X., Xue, N. and Han, Z., 2021. A meta-analysis of heavy metals pollution in farmland and urban soils in China over the past 20 years. Journal of Environmental Sciences, 101, pp.217-226.

Zaynab, M., Al-Yahyai, R., Ameen, A., Sharif, Y., Ali, L., Fatima, M., Khan, K.A. and Li, S., 2022. Health and environmental effects of heavy metals. Journal of King Saud University-Science, 34(1), p.101653.